

AD-A051 554

NAVAL UNDERSEA WARFARE CENTER SAN DIEGO CALIF
NEW MODELS FOR SHALLOW WATER PROPAGATION.(U)
JAN 68 H P BUCKER, H E MORRIS
NUWC-TN-45

F/6 17/1

UNCLASSIFIED

NL

| OF |
AD
A051 554



END
DATE
FILMED
4-78
DDC

001837

AD A051554

3rd MOST Project

00 U1B

Library

NUWC-TN-45

14

1

NAVAL UNDERSEA WARFARE CENTER

11

JAN ~~1968~~ 1968

12

24p.

Good

9 Technical notes

6

NEW MODELS FOR SHALLOW WATER PROPAGATION

10

by H.P. Bucker & H.E. Morris

San Diego, California

16 F10103

17

SF1010315

SUBPROJECT NO. SF1010315

TASK NO. 8105

45

001837

Apr 10

DISTRIBUTION STATEMENT A

Approved for public release
Distribution Unlimited

DDC


RECEIVED
MAR 21 1978
RECEIVED

403 023

AB

ABSTRACT

Several new and improved shallow-water normal-mode models have been developed to represent the shallow-water area encountered on the FASOR I and II cruises. These models include a "linear" gradient velocity profile, an Epstein velocity profile, and a profile with three "linear" gradient segments. In all cases a layered viscoelastic bottom is used. Generally good agreement is shown between the calculated and experimental measurements of propagation loss on the FASOR stations. This memorandum has been prepared because it is believed that the information may be useful in this form to others at NUWC and to a few persons outside NUWC. This memorandum should not be construed as a report since its function is to present information that later will be supplemented and expanded in a report.

ACCESSION for	
NTIS	Write Section <input checked="" type="checkbox"/>
BDC	Read Section <input type="checkbox"/>
UNANNOUNCED	<input type="checkbox"/>
JUSTIFICATION	
<i>per ltr on file</i>	
BY	
DISTRIBUTION/AVAILABILITY CODES	
Dist.	AVAIL. and SPECIAL
	

INTRODUCTION*

For shallow water propagation at moderate sea states the most important environmental factors are the nature of the bottom and the sound velocity profile. At NUWC, San Diego, we have worked to develop models that accurately represent the profile and the bottom sediments. We will use these models for calculations of propagation in certain areas of interest, as checks for approximate shallow water models, and to study special aspects of propagation such as the effect of the thermocline.

We will present two models. In one model there are either one or three water layers where the square of the index of refraction is a linear function of depth. Since the velocity is almost a linear function with depth we will call this a linear gradient model. This type of profile has been used by Marsh¹, Tolstoy², Pedersen³, and others in other normal mode calculations. The second model is a one layer Epstein profile. Since general normal mode theory is in the literature we will only touch on the unique features of the present models.

*This technical note includes part of the information presented as Paper G-8, 25th U. S. Navy Symposium on Underwater Acoustics, Orlando, Florida, November 7-9, 1967. This work was accomplished under NAVSHIPS Sub-project SF 101 03 15 Task 8105.

LINEAR GRADIENT MODEL

Figure 1 shows the potential functions for a single linear gradient model.

The functions h_1 and h_2 are modified Hankel functions of order one-third.⁴ The bottom is made up of an arbitrary number of viscoelastic layers. In order to use an old computer subroutine that calculates the reflection coefficient for this type of bottom, a pseudo constant-velocity water layer is set in between the depths designated z_b' and z_b . After the usual interface conditions are set, we let z_b' approach z_b so that the iso-velocity layer disappears from the problem.

The argument of the modified Hankel function, η , is a function of the mode wave number k and z . The parameters a and R are functions of k .

Finding the modes is the mathematical problem determining that set of k 's which satisfy all boundary conditions. For example, we can use the boundary conditions at $z = z_b'$ to fix A and B . The mode condition, also called the dispersion equation, can then be written as the condition that the potential be zero at the surface, $z = 0$. The dispersion equation is stated in Figure 2.

The asymptotic form of the range dependent part of the potential function contains the term e^{ikr} . Thus the real part of k determines the horizontal phase velocity of a mode and the imaginary part of k fixes the attenuation. n denotes the mode number. If we equate the real part of k with ω/c_n' , where c_n' is the horizontal phase velocity of a ray in the channel, we can make a connection between ray and mode theory that will prove helpful in the solution and in the interpretation of

the results. The value of c_n' is set by requiring the ray to satisfy a constructive interference relation⁵ as it travels down the channel. As shown in Figure 2, X is the horizontal cycle distance, T is the time to complete a cycle, ω is the angular frequency, ϵ_b is the phase shift on bottom reflection, ϵ_s is the $-\pi/2$ for a turn-over, or $-\pi$ if the ray reflects from the surface, and n is the mode number. The approximate value of the imaginary part of the phase velocity is calculated by noting the loss per bottom reflection then distributing this loss as an exponential function of r .⁶

The solutions of the exact and approximate dispersion equation are shown in Figure 3. We have plotted values of mode velocity $c_n = \omega/k_n$ rather than the k_n so that the real part of c_n can be associated with the horizontal phase velocities of the associated rays as shown in Figure 2. For example, if the real part of c_n is close to the velocity at the bottom of the channel the mode will be confined to depths where the sound velocity is less than the real part of c_n . When the real part of c_n is equal to the surface velocity the mode begins to reflect from the surface and the attenuation goes up because the cycle distance X begins to diminish in length.

The open circles in Figure 3 are the approximate values of phase velocity and the crosses are exact values. The two sets of c_n are essentially identical except for three of the modes. Note that the first 15 modes, those which don't reflect from the surface, have about the same attenuation. This is because as the mode number goes up the bottom loss goes up but the distance between reflections also becomes

greater. This effect of loss independent of grazing angle was used by Urick⁷ in his shallow water ray theory model. Later, results will be discussed for a 3 layer linear gradient case. The theory is essentially the same as for the single layer model.

EPSTEIN MODEL

The second model concerns a one layer Epstein profile as shown in Figure 4. The case here is a transition layer with the same surface and bottom velocities as in the linear gradient model. The profile may also contain a hyperbolic secant term, however this case will not be discussed.

The solution is similar to the linear gradient model except the potential function is now a product of an exponential term times a hypergeometric function. The exact form of these terms can be found in a paper by Deavenport⁸.

Values of phase velocity for this profile are shown in Figure 5. In this case the mode attenuation increases as the bottom loss increases but then has a sharp decrease as the phase velocity approaches the sound velocity in the upper part of the channel. The result is two sets of low attenuation modes. The first group strong below the thermocline and the second set strong above. Thus propagation across the thermocline suffers. For the present values of surface and bottom velocity and the case of an extremely sharp thermocline (two iso-velocity layers) the loss across the thermocline is 5 to 10 db. This is at 1.5kHz, the loss would be greater at higher frequencies. The rule is: don't cross your modes in the middle of a propagation run.

MODE SUMMATION

To calculate the sound field the modes are summed as shown in Figure 6. The second form of the normalizing term N_n can generally be calculated with better accuracy because it is dependent upon ϕ calculated throughout the channel, rather than only at the surface. To facilitate the integration of ϕ^2 over the sediment layers we use a trick as shown in Figure 7.

Taking the modes one at a time, we pick an absorbing liquid half-space that has the same density as the water and will give the same reflection coefficient. That is, the layered-viscoelastic bottom is used to find the modes but we switch to an absorbing-liquid half-space for the normalization. The integral from z_b to ∞ can be completed by inspection since there is only an exponential wave in the absorbing liquid.

RESULTS - 3 LAYER LINEAR GRADIENT MODEL

There were three shallow water stations on the last FASOR cruise in the Pacific by NUWC. On one of these the two iso-velocity layer model provided a good fit to the velocity profile. On the other two stations, OAK and THORN, we have made intensity calculations using a three layer linear gradient model. In Figure 8 are ET's taken at the time of the tests for station OAK. The tests extended over 17 hours. The broader, heavier line is our fit to the profile.

Measured and calculated values of propagation loss for ranges up to 50 kyd are shown in Figure 9. Thorpe's value of volume attenuation¹⁰ and Amos values of surface loss for sea state 1 were added.

That is, we calculated propagation loss from Marsh and Shulkin's⁹ equations for sea state 1 and sea state 0. The difference was taken as the surface loss. The agreement between calculated and experimental results is somewhat better than we reported last year using a two layer iso-velocity model. However, the experimental losses are about 6 db greater over the section of the range interval from 20 to 40 kyd.

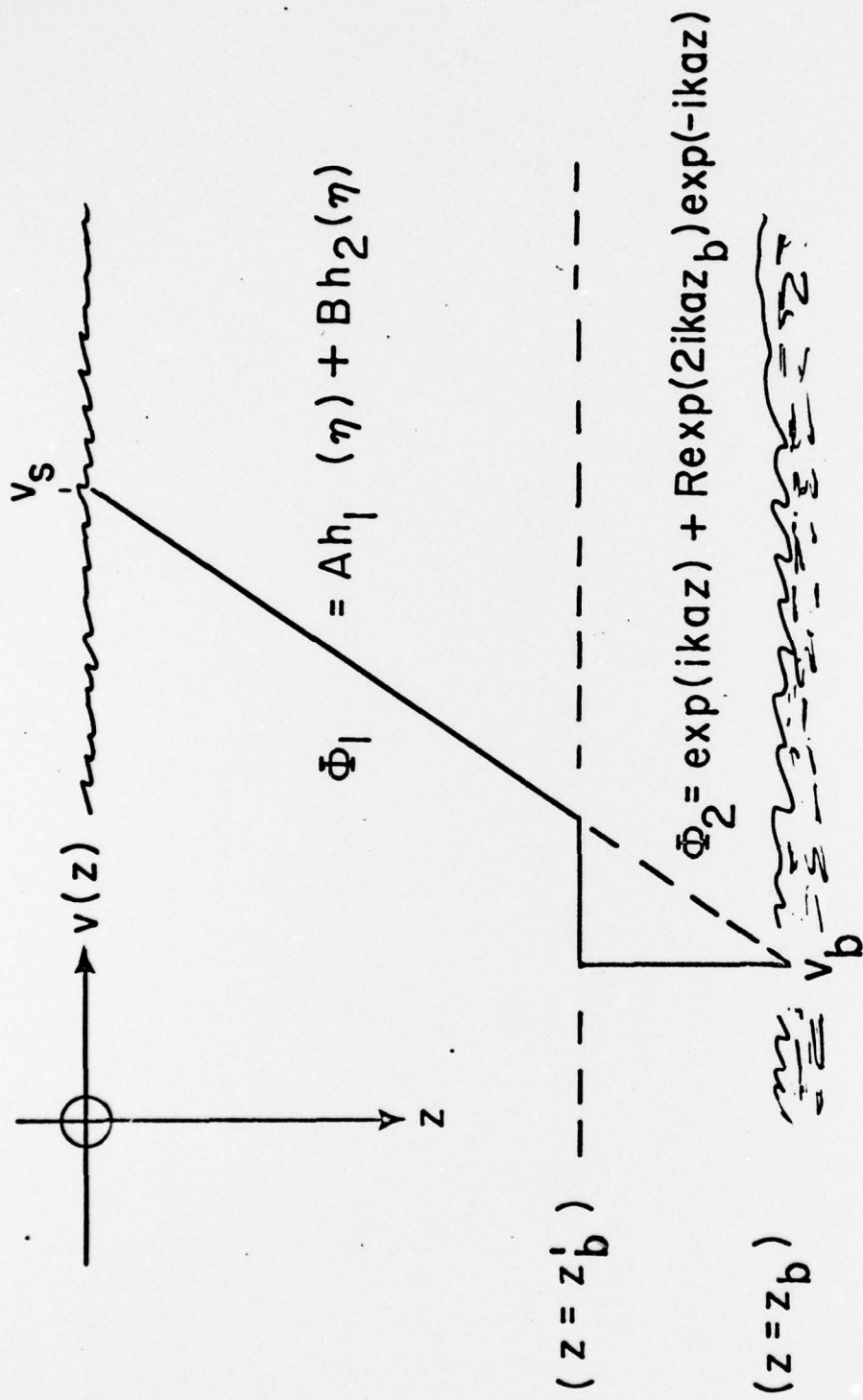
The BT's and the three layer model for THORN are shown in Figure 10. The profile is interesting because of the well developed surface duct. The modes separate naturally into three groups. A set that corresponds to rays that have only bottom reflections, two modes in the surface duct, and a group of higher order modes that reflect alternately from the surface and bottom. The mode phase velocities are shown in Figure 11. Again the approximate roots are an accurate estimate of the real parts of the set of c_n 's for all modes and of the imaginary parts for all modes but one. The calculated and observed values of propagation loss, Figure 12, can be seen to be in good agreement.

CONCLUSION

With the present models we feel that a satisfactory first order theory has been developed for shallow water propagation. On this framework additions can be added to account for boundary roughness, horizontal variations, and other second order effects.

REFERENCES

1. H. W. Marsh, "Theory of Anomalous Propagation of Acoustic Waves in the Ocean", USNUSL Report No. 111 (1950).
2. Ivan Tolstoy, "Guided Waves in a Fluid with Continually Variable Velocity Overlying an Elastic Solid: Theory and Experiment", JASA, 32, 81-87, (1960).
3. M. A. Pedersen and D. F. Gordon, "Normal Mode Theory Applied to Short Range Propagation in an Underwater Acoustic Surface Duct", JASA 37, 105-118 (1965).
4. Tables of the Modified Hankel Functions of Order One-third and of Their Derivatives. Harvard University Press, Cambridge Mass. (1945).
5. H. P. Buckner, "Normal Mode Propagation in Shallow Water", JASA, 36, 251-258 (1964).
6. E. T. Kornhauser and W. P. Raney, "Attenuation in Shallow Water Propagation due to an Absorbing Bottom", JASA, 27, 689-692 (1955).
7. R. J. Urick, "A Prediction Model for Shallow Water Sound Transmission", Naval Ordnance Laboratory. TR 67-12 (February 1967).
8. R. L. Deavenport, Radio Science, Vol. 1, 709-724 (1966).
9. H. W. Marsh and M. Schulkin, "Shallow-Water Transmission, (L)", JASA, 34, 863-864 (1962).
10. William H. Thorpe, "Analytic Description of the Low-Frequency Attenuation Coefficient, (L)", JASA, 42, 270 (1967).



Velocity Profile: $v(z)^{-2} = v_s^{-2} (1 + bz)$

FIGURE 1

EXACT DISPERSION EQ.:

$$\Phi_1(z=0, k=k_n) = 0, n=1, 2, 3, \dots$$

APPROXIMATE DISPERSION EQ.:

$$k_n = \omega/c_n \approx \omega/(c_n' - ic_n'')$$

$$\omega(T - X/c_n') + \epsilon_b + \epsilon_s = (n-1)2\pi$$

$$c_n'' = (c_n')^2 \cdot BL / (x \cdot \omega \cdot 8.686)$$

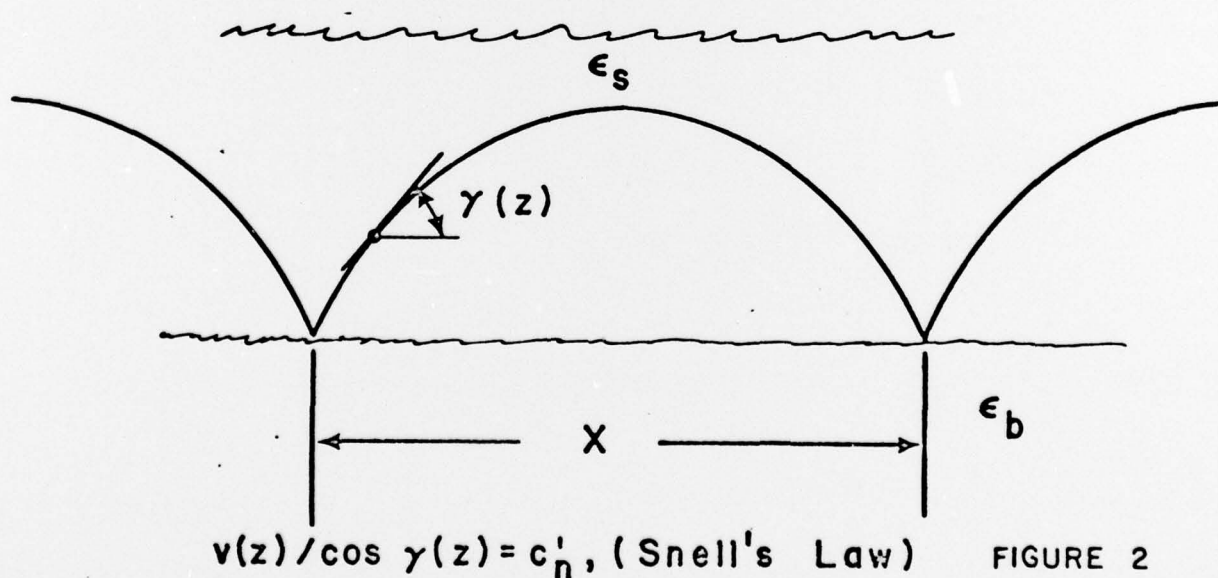


FIGURE 2

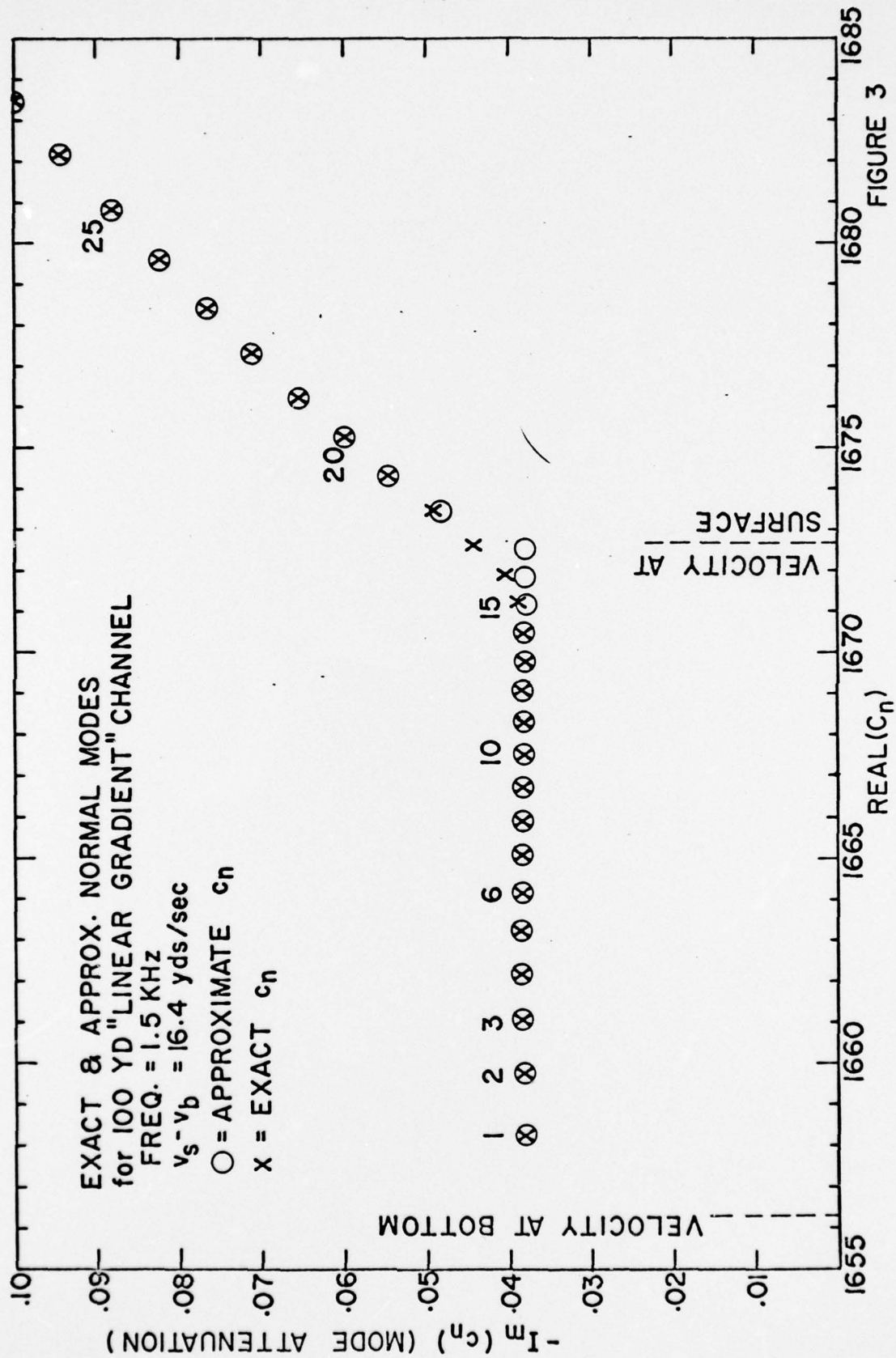
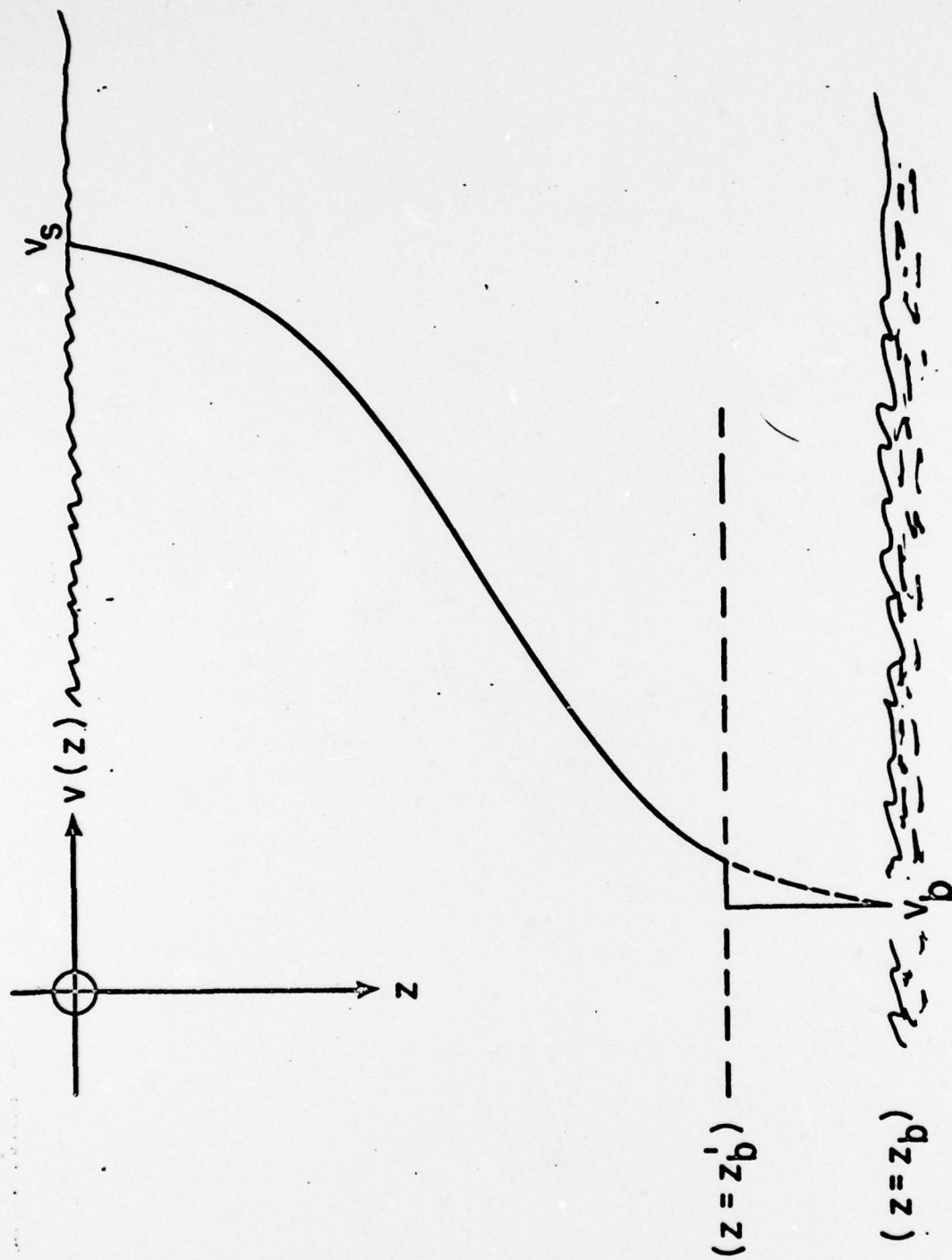
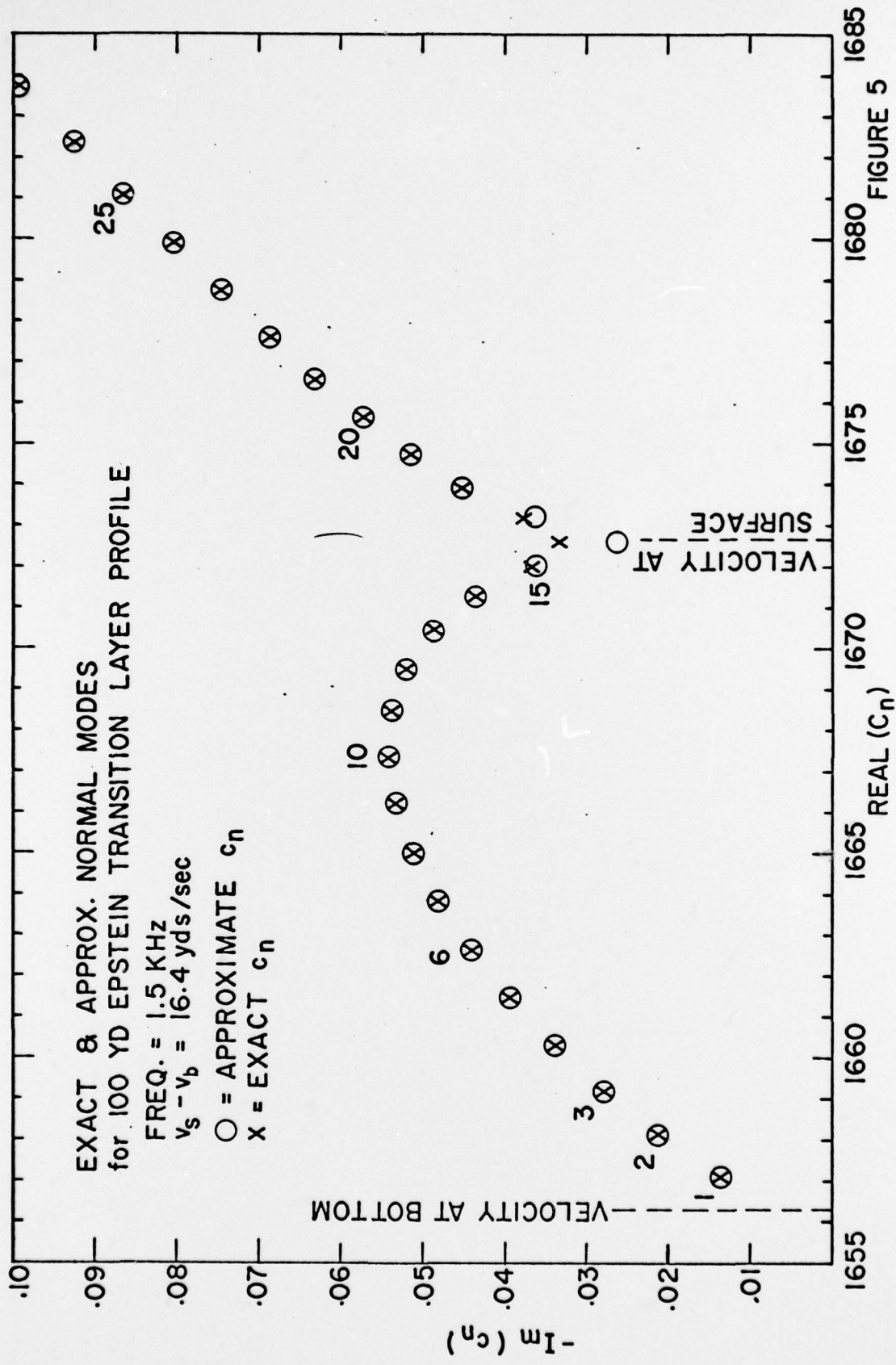


FIGURE 3



Velocity Profile: $v(z)^{-2} = A \tanh\left(\frac{z-a}{b}\right) + D$

FIGURE 4



1685
1680
1675
1670
1665
1660
1655

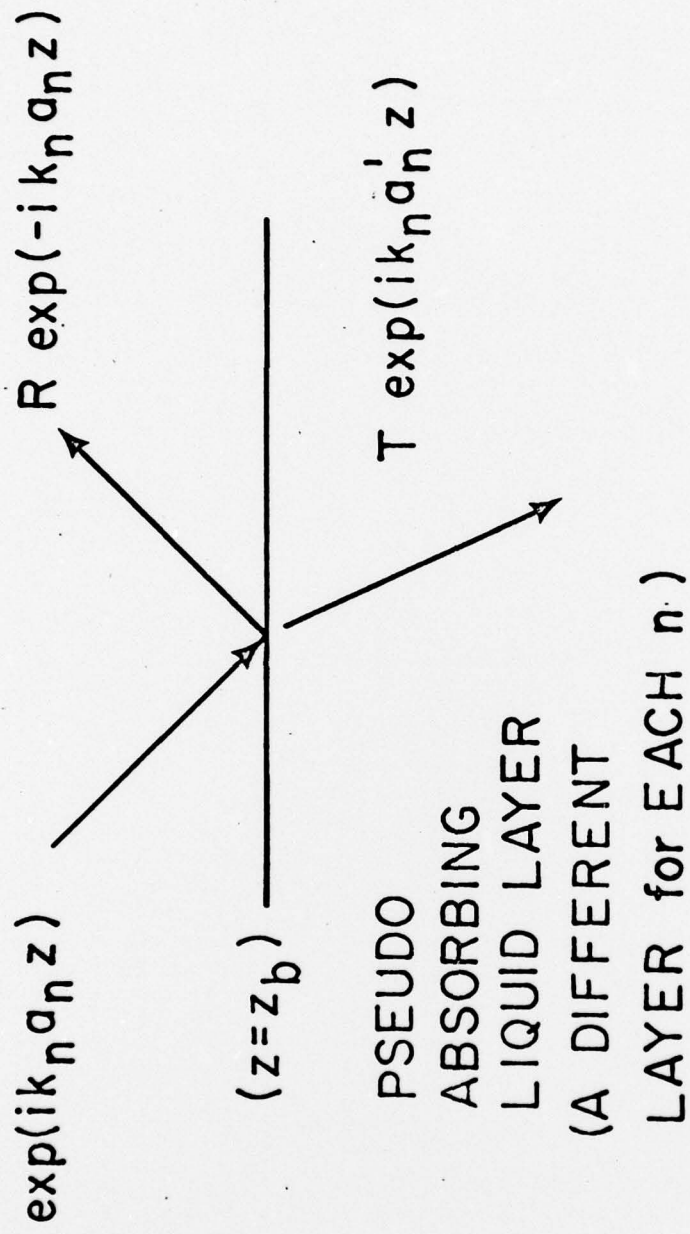
FIGURE 5

$$\Phi = (2\pi/r)^{\frac{1}{2}} \sum_n N_n \phi_n(z_0) \phi_n(z) e^{iknr}$$

$$N_n = \begin{cases} 2(k_n)^{\frac{1}{2}} / (\partial\phi/\partial z \cdot \partial\phi/\partial k) |_{z=0, k=k_n} \\ 1 / [(k_n)^{\frac{1}{2}} \int_0^\infty \phi_n^2 dz] . \end{cases}$$

$$\text{PROPAGATION LOSS} = -10 \log_{10} |\Phi|^2$$

FIGURE 6



$$a'_n = (1 - R) / (1 + R)$$

$$T = 2 a_n / (a_n + a'_n)$$

FIGURE 7

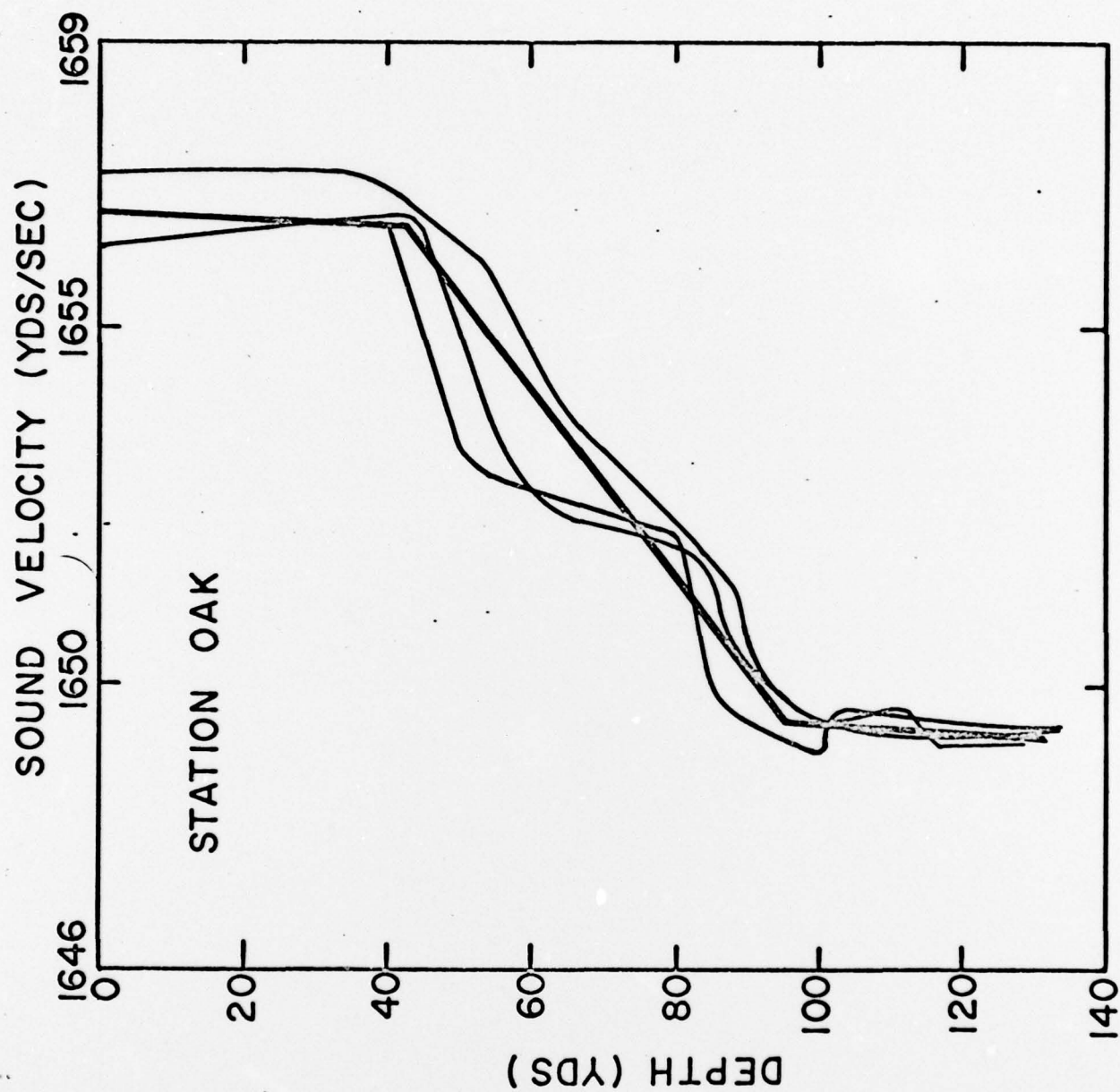


FIGURE 8

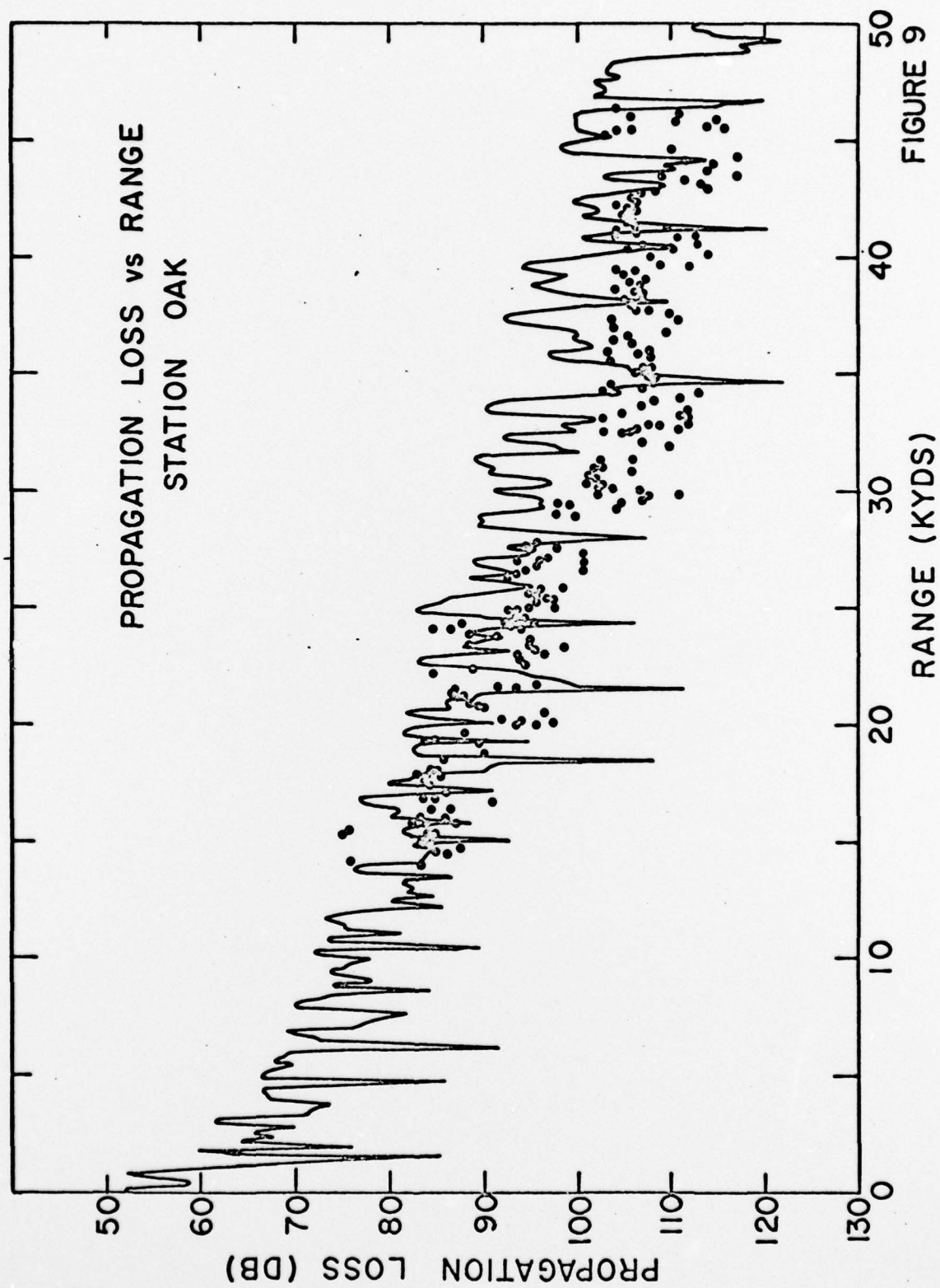


FIGURE 9

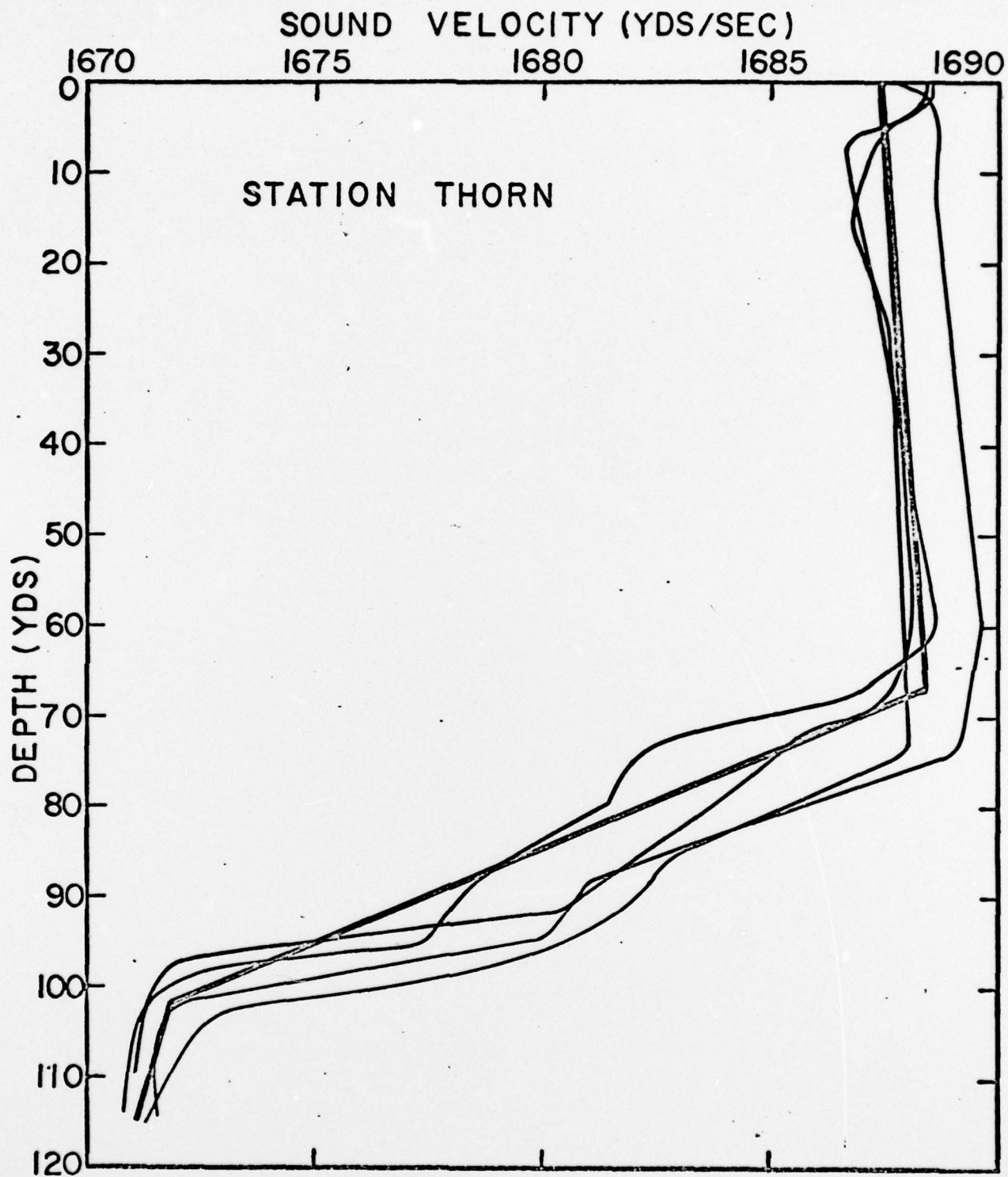


FIGURE 10

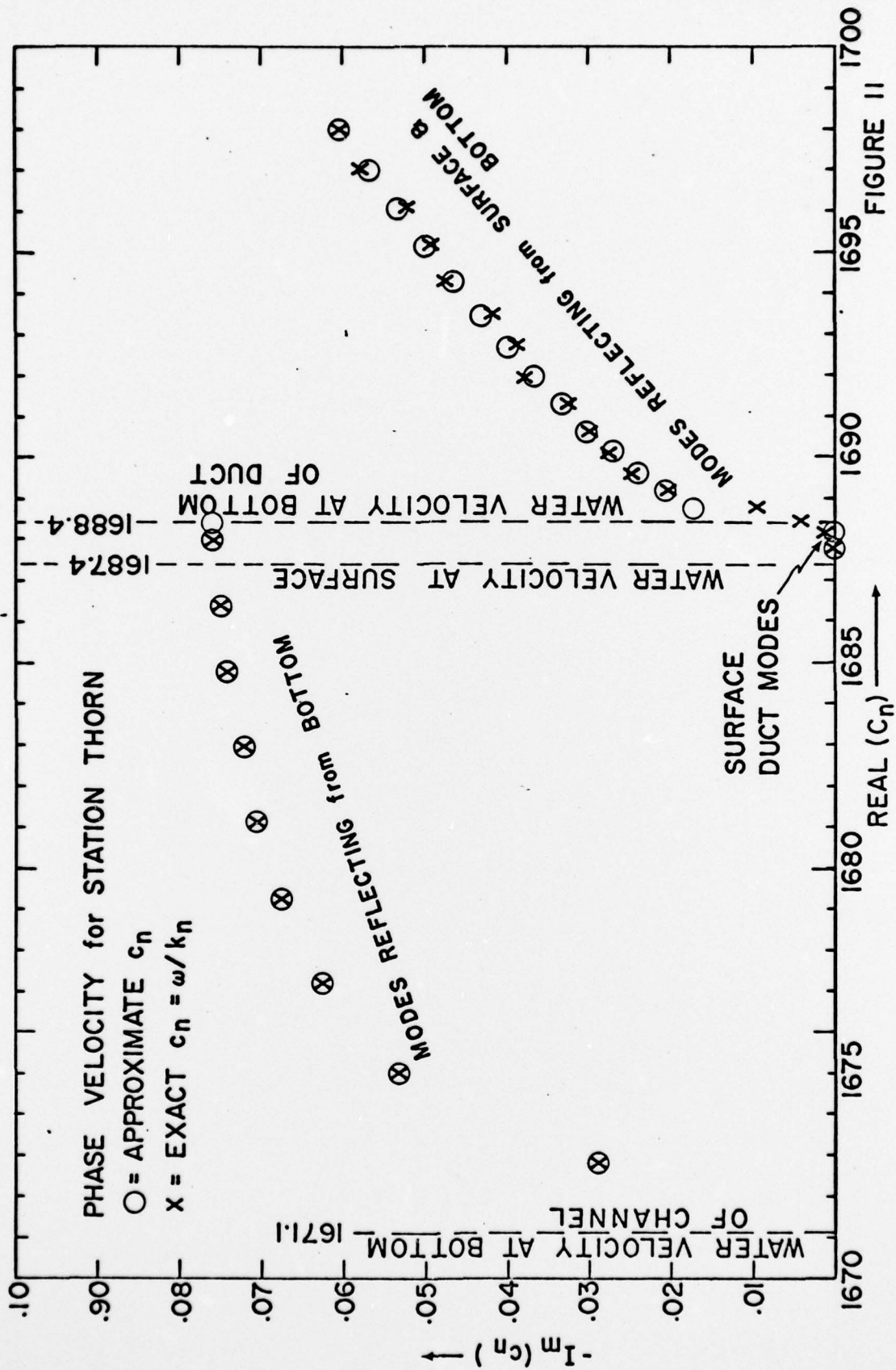


FIGURE 11

